

**Supplementary Information for**

**Novel Mn-Bi-S hybrid mesoporous nanosheets as efficient  
electrocatalyst for nitrogen reduction reaction**

Yining Ban,<sup>a</sup> Zizai Ma,<sup>b,c,\*</sup> Zihao Wan,<sup>a</sup> Hefeng Yuan<sup>a,d</sup> and Xiaoguang Wang<sup>a,c,\*</sup>

<sup>a</sup> Laboratory of Advanced Materials and Energy Electrochemistry, Institute of New Carbon Materials, College of Material Science and Engineering, Taiyuan University of Technology, Taiyuan, 030024, China. E-mail: [wangxiaog1982@163.com](mailto:wangxiaog1982@163.com)

<sup>b</sup> College of Chemistry, Taiyuan University of Technology, Taiyuan, 030024, China. E-mail: [mazizai@tyut.edu.cn](mailto:mazizai@tyut.edu.cn)

<sup>c</sup> Shanxi Key Laboratory of Gas Energy Efficient and Clean Utilization, Taiyuan University of Technology, Taiyuan, 030024, China.

<sup>d</sup> Institute of Resources and Environmental Engineering, Shanxi University, Taiyuan 030006, China.

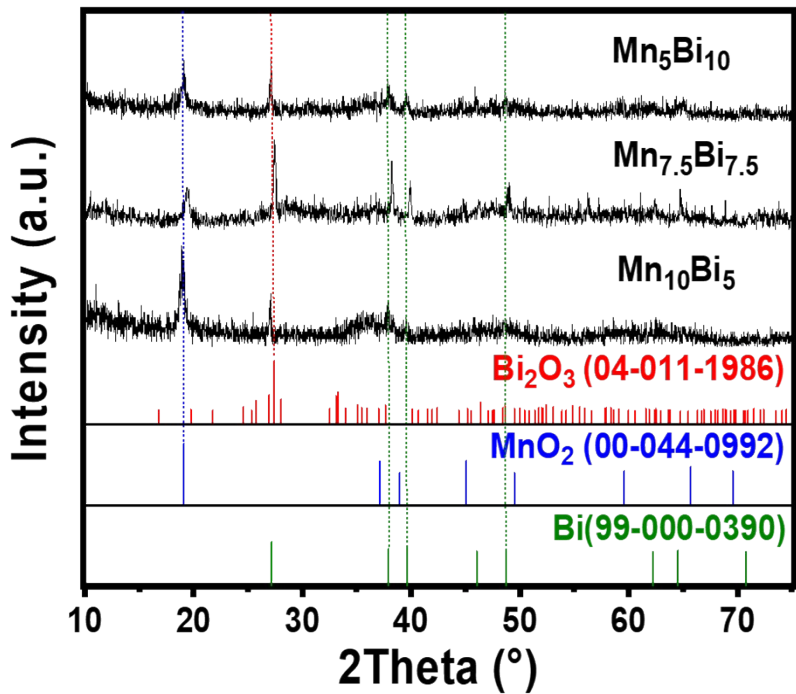


Fig. S1 XRD patterns of  $\text{Mn}_5\text{Bi}_{10}$ ,  $\text{Mn}_{7.5}\text{Bi}_{7.5}$  and  $\text{Mn}_{10}\text{Bi}_5$ .

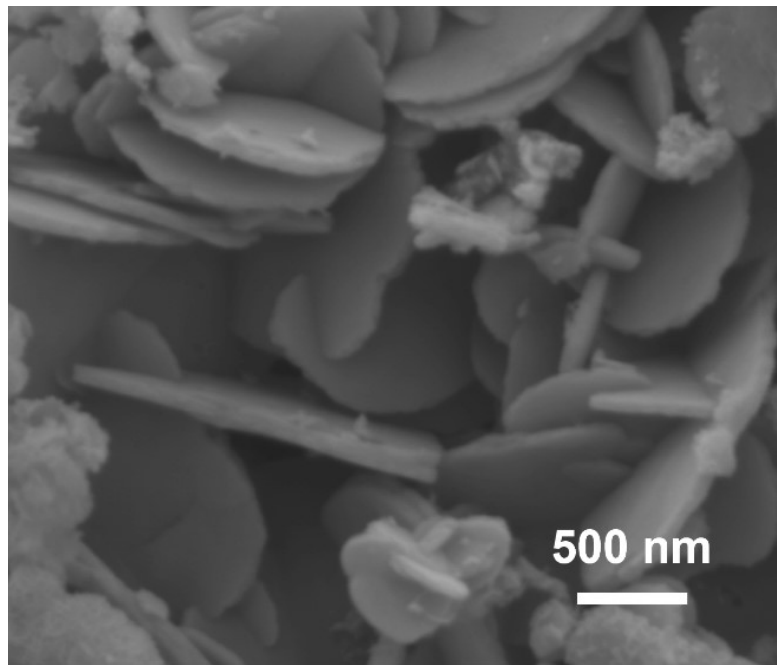


Fig. S2 SEM image of Mn<sub>7.5</sub>Bi<sub>7.5</sub>.

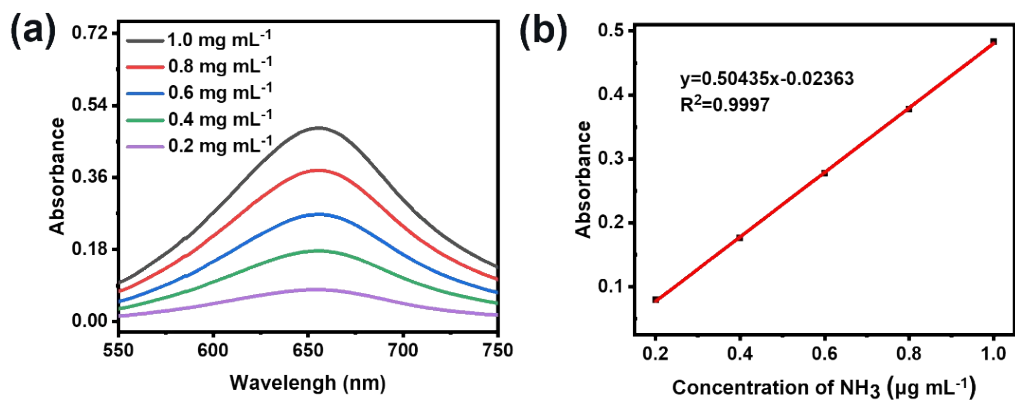


Fig. S3 (a) UV-vis spectra of indophenol assays with  $\text{NH}_4^+$  after incubated for 2 h at room temperature. (b) Calibration curve used for estimation of concentration of  $\text{NH}_4\text{Cl}$ .

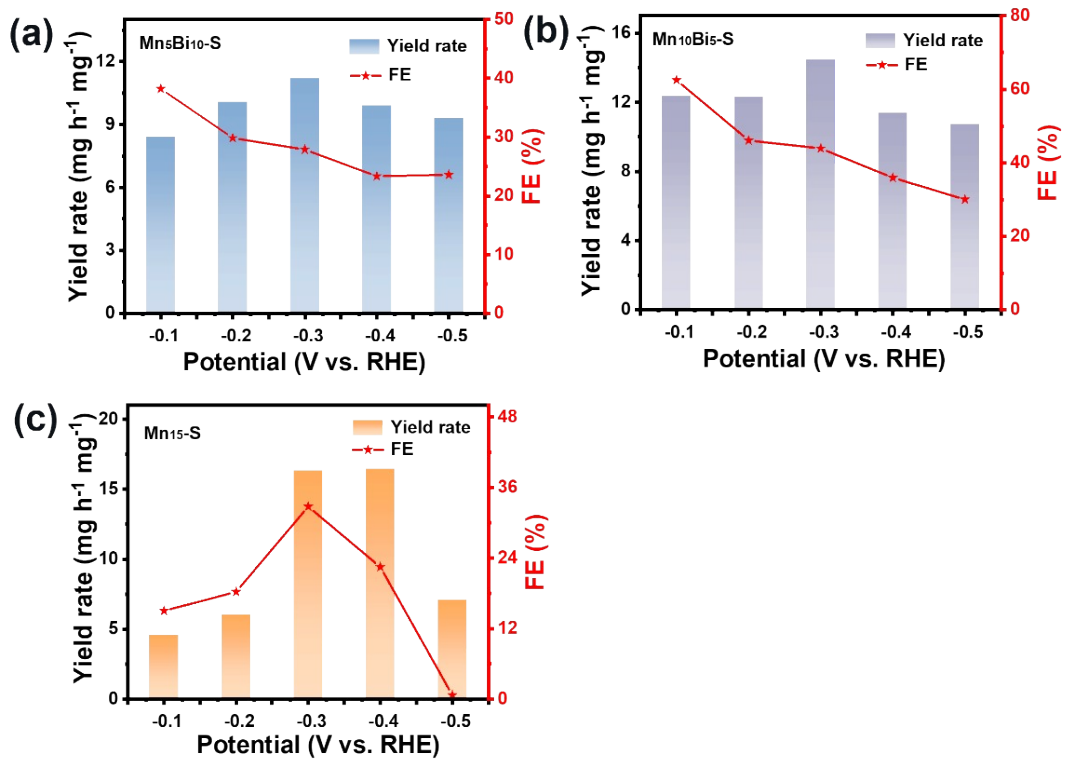


Fig. S4 Average ammonia production rate and FE at different potentials from -0.1 V to -0.5 V vs. RHE. (a) Mn<sub>5</sub>Bi<sub>10</sub>-S, (b) Mn<sub>10</sub>Bi<sub>5</sub>-S and (c) Mn<sub>15</sub>-S.

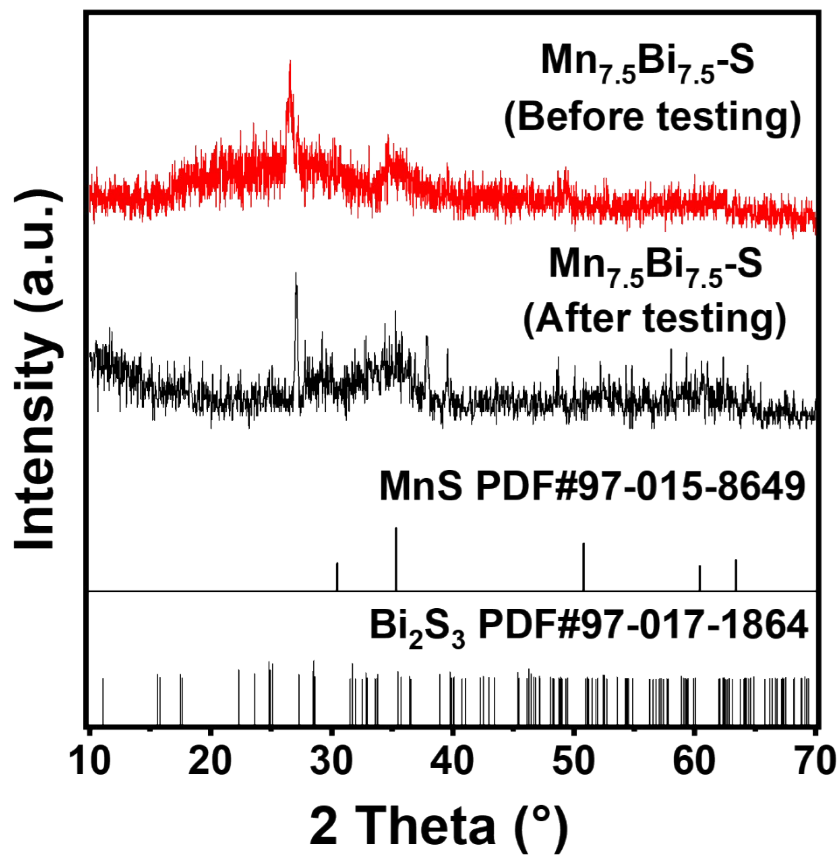


Fig. S5 XRD patterns of  $\text{Mn}_{7.5}\text{Bi}_{7.5}\text{-S}$  catalyst before and after stability test.

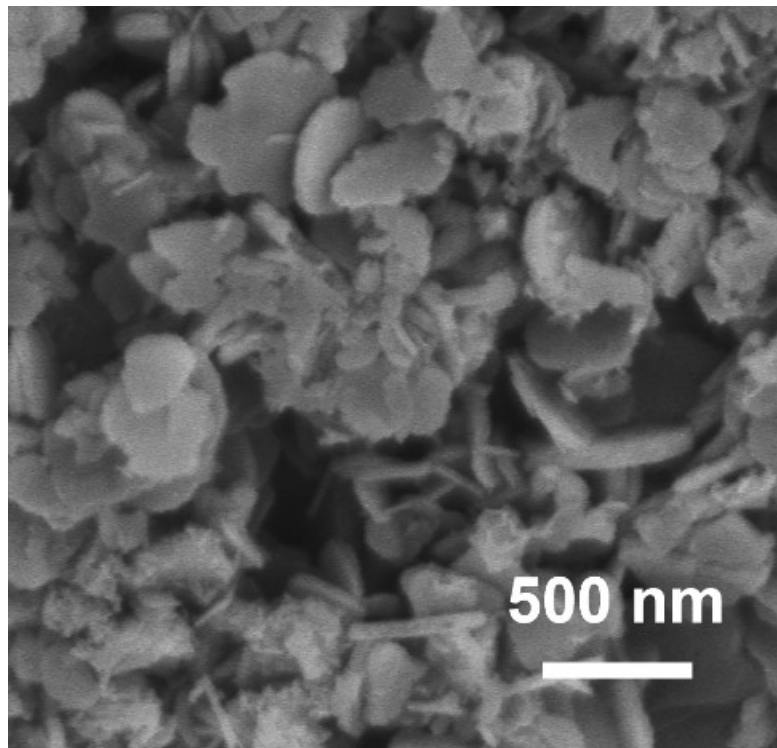


Fig. S6 SEM image of Mn<sub>7.5</sub>Bi<sub>7.5</sub>-S catalyst after stability test.

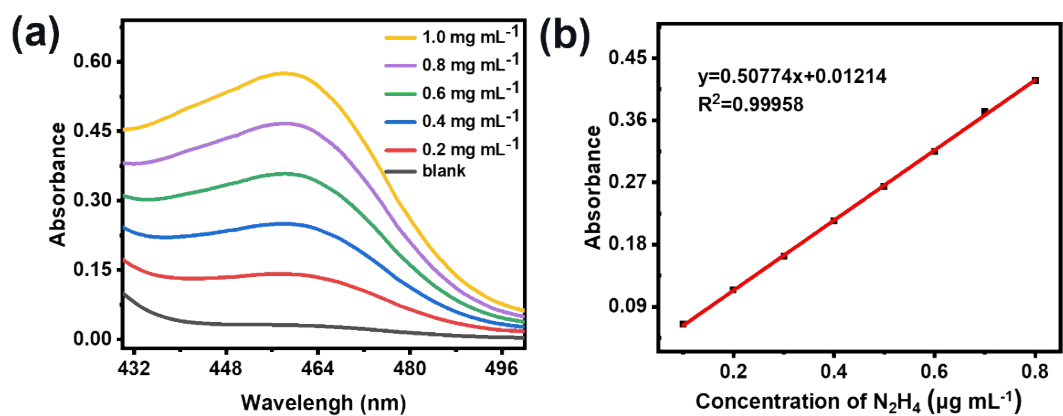


Fig. S7 (a) UV-vis spectra of various  $\text{N}_2\text{H}_4$  concentrations after incubated for 15 min at room temperature. (b) Calibration curve used for calculation of  $\text{N}_2\text{H}_4$  concentrations.

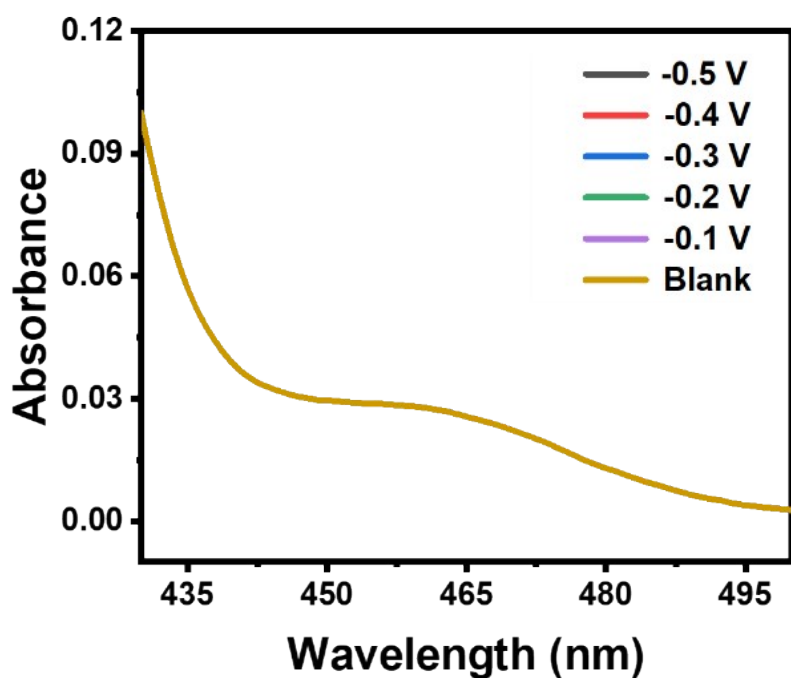


Fig. S8 UV-vis spectra of the electrolytes stained with Watt and Chrisp indicator at various potentials for 2 h.

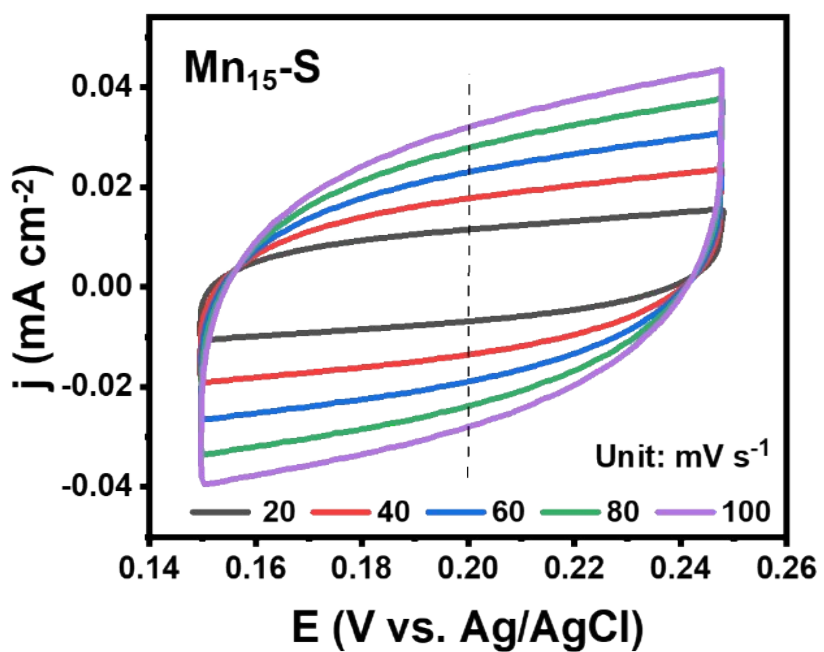


Fig. S9 CV scans measured at a potential range from 0.15 to 0.25 V vs. Ag/AgCl with different scan rates ( $20, 40, 60, 80$  and  $100 \text{ mV s}^{-1}$ ) for  $\text{Mn}_{15}\text{-S}$ .

**Table S1** Optimal yield rate and Faraday efficiency of  $\text{Mn}_x\text{Bi}_{15-x}\text{-S}$  ( $x = 5, 7.5, 10, 15$  at. %).

Catalyst	Yield rate ( $\mu\text{g h}^{-1} \text{mg}^{-1}$ )	FE (%)
<b>Mn<sub>7.5</sub>Bi<sub>7.5</sub>-S</b>	21.56	73.36
<b>Mn<sub>7.5</sub>Bi<sub>7.5</sub></b>	15.94	40.06
<b>Mn<sub>10</sub>Bi<sub>5</sub>-S</b>	14.48	43.91
<b>Mn<sub>5</sub>Bi<sub>10</sub>-S</b>	11.18	27.87
<b>Mn<sub>15</sub>-S</b>	16.31	32.77

**Table S2** Comparison for the NRR electrocatalytic activity of  $\text{Mn}_{7.5}\text{Bi}_{7.5}\text{-S}$  catalyst with other reported catalysts.

Catalyst	Electrolytes	Yield rate	FE	Ref.
<b>Mn-Bi<sub>2</sub>O<sub>3</sub></b>	0.1 M Na <sub>2</sub> SO <sub>4</sub>	23.54 $\mu\text{g h}^{-1} \text{mg}^{-1}$	21.63%	<sup>1</sup>
<b>CuMn</b>	0.1 M Na <sub>2</sub> SO <sub>4</sub>	28.9 $\mu\text{g h}^{-1} \text{mg}^{-1}$	9.83%	<sup>2</sup>
<b>BQD/15MS</b>	0.1 M Na <sub>2</sub> SO <sub>4</sub>	18.5 $\mu\text{g h}^{-1} \text{mg}^{-1}$	33.2%	<sup>3</sup>
<b>Bi<sub>2</sub>S<sub>3-x</sub>/Ti<sub>3</sub>C<sub>2</sub>T<sub>x</sub></b>	0.1 M Na <sub>2</sub> SO <sub>4</sub>	68.3 $\mu\text{g h}^{-1} \text{mg}^{-1}$	22.5%	<sup>4</sup>
<b>Bi NS</b>	0.1 M Na <sub>2</sub> SO <sub>4</sub>	13.23 $\mu\text{g h}^{-1} \text{mg}^{-1}$	10.46%	<sup>5</sup>
<b>Bi@C</b>	0.1 M Na <sub>2</sub> SO <sub>4</sub>	4.22 $\mu\text{g h}^{-1} \text{mg}^{-1}$	15.10%	<sup>6</sup>
<b>S-Bi NB</b>	0.1 M Na <sub>2</sub> SO <sub>4</sub>	10.28 $\mu\text{g h}^{-1} \text{mg}^{-1}$	10.48%	<sup>7</sup>
<b>Au/PCN</b>	0.05 M H <sub>2</sub> SO <sub>4</sub>	13.8 $\mu\text{g h}^{-1} \text{cm}^{-2}$	61.8%	<sup>8</sup>
<b>AuNPs</b>	0.1 M Li <sub>2</sub> SO <sub>4</sub>	9.22 $\mu\text{g h}^{-1} \text{cm}^{-2}$	73.32%	<sup>9</sup>
<b>Bi-NPs</b>	0.1 M Na <sub>2</sub> SO <sub>4</sub>	16.25 $\mu\text{g h}^{-1} \text{mg}^{-1}$	12.11 %	<sup>10</sup>
<b>Mn<sub>7.5</sub>Bi<sub>7.5</sub>-S</b>	0.1 M Na <sub>2</sub> SO <sub>4</sub>	21.56 $\mu\text{g h}^{-1} \text{mg}^{-1}$	73.36%	This work

## Notes and references

1. H. Ying, J. H. Bi, H. Xu, G. B. Wu, X. N. Wu, J. C. Hao and Z. H. Li, *ACS Sustain. Chem. Eng.*, 2022, **10**, 6766-6774.
2. Y. H. Cui, A. Q. Dong, Y. B. Qu, J. Y. Zhang, M. Zhao, Z. L. Wang and Q. Jiang, *Chem. Eng. J.*, 2021, **426**, 6.
3. N. Gao, H. M. Yang, D. Dong, D. Y. Dou, Y. J. Liu, W. J. Zhou, F. F. Gao, C. Nan, Z. H. Liang and D. H. Yang, *J. Colloid Interface Sci.*, 2022, **611**, 294-305.
4. Y. J. Luo, P. Shen, X. C. Li, Y. L. Guo and K. Chu, *Nano Res.*, 2022, **15**, 3991-3999.
5. L. Q. Li, C. Tang, B. Q. Xia, H. Y. Jin, Y. Zheng and S. Z. Qiao, *ACS Catalysis*, 2019, **9**, 2902-2908.
6. Y. C. Wan, H. J. Zhou, M. Y. Zheng, Z. H. Huang, F. Y. Kang, J. Li and R. T. Lv, *Adv. Funct. Mater.*, 2021, **31**, 10.
7. Y. X. Lin, L. Yang, H. L. Jiang, Y. K. Zhang, Y. N. Bo, P. Liu, S. M. Chen, B. Xiang, G. Li, J. Jiang, Y. J. Xiong and L. Song, *J. Phys. Chem. Lett.*, 2020, **11**, 1746.
8. K. Peramaiah, V. Ramalingam, H. C. Fu, M. M. Alsabban, R. Ahmad, L. Cavallo, V. C. Tung, K. W. Huang and J. H. He, *Adv. Mater.*, 2021, **33**, 12.
9. Y. Zhou, X. P. Yu, X. Y. Wang, C. Chen, S. T. Wang and J. Zhang, *Electrochim. Acta*, 2019, **317**, 34-41.
10. D. Z. Yao, C. Tang, L. Q. Li, B. Q. Xia, A. Vasileff, H. Y. Jin, Y. Z. Zhang and S. Z. Qiao, *Adv. Energy Mater.*, 2020, **10**, 8.